

It is natural that the drag of the plate at the limit remains the same, while the magnitude of the reverse flow may be fairly arbitrary but remain within the limits  $0 < \delta \leq \pi/[2(\pi + 4)]$ , i.e., be bounded above by the "Éfros" value. If  $h \sim c^\alpha$  ( $\alpha > 2$ ) and  $c \rightarrow 0$ , then  $\delta_* = 0$ ,  $d_* \rightarrow \infty$ .

We thank G. I. Taganov for initiating this investigation.

#### LITERATURE CITED

1. M. I. Gurevich, Theory of Jets of an Ideal Fluid [in Russian], Nauka, Moscow (1979).

#### USE OF THE MODEL OF A SECOND DISSIPATIVE LAYER AND A WAKE TO DESCRIBE QUASISTEADY CAVITATIONAL FLOW ABOUT A FLAT PLATE

G. I. Taganov

UDC 532.527

The model of a second dissipative layer and a wake in [1] was used for steady flow of a viscous incompressible fluid about a flat plate within a large range of angles of attack  $\alpha_{cr} < \alpha < 90^\circ$  [2]. Comparison of the relations  $c_x = f(\alpha)$  and  $c_y = f(\alpha)$  obtained in [2] (see [3] also) with experimental data showed that the model underestimates  $c_x$  and  $c_y$  in this range by about 15%. This underestimation was explained in [2] by the fact that the distinctly nonsteady flow seen under experimental conditions is replaced by a quasisteady flow in the model. Moreover, the model does not consider the energy associated with pulsative motion in the near wake, which was directly confirmed experimentally in [4]. The suppression of nonsteady pulsations behind a flat plate (the experimentally-fixed reduction in the frequency of vortex shedding) in a flow at an angle  $\alpha = 90^\circ$  through the use of a splitter plate of roughly chord length located along the symmetry plane of the flow in the separation zone also leads to a reduction in  $c_x$  by about 15% at the limit, i.e., to as close an agreement between the theory and experiment as can be expected from a hydrodynamic model. If we consider that the problem of theoretically determining the drag of a flat plate located perpendicular to an incoming flow has attracted the attention of physicists and hydrodynamicists for the last two centuries, then the success of the model of a second dissipative layer and wake in regard to the solution of this problem offers hope and grounds for use of the model to solve a related hydrodynamic problem (the subject of the present investigation) – theoretical determination of the resistance force acting on a plate in a separated cavitation flow as a function of the determining parameter – the cavitation number  $Q = 2(p_\infty - p_c)/\rho v_\infty^2$  ( $p_c$  is the pressure in the cavity behind the plate).

There arises the question of the need for a new (energy) approach to an old hydrodynamic problem which was theoretically described by the middle of the present century by any of four mathematical models. While differing somewhat from each other at  $Q \neq 0$ , at  $Q \rightarrow 0$  these models approach the classical Helmholtz–Kirchhoff model  $c_x = 2\pi/(\pi + 4) \simeq 0.88$  and are in fair agreement with the experimental data in the range of cavitation numbers  $0 < Q < 1.0$ .

Let us discuss the considerations which motivated us to develop a new approach.

First, it has long been known that separated cavitation flow is nonsteady and that it is not possible to construct a steady flow of an incompressible fluid which can reliably describe the flow observed experimentally at  $Q \neq 0$  without contradicting physical reality. Since the well-known mathematical models of flow about a plate at  $Q \neq 0$  are steady-state models, the drag values obtained from them can, strictly speaking, be regarded only as conditional. This conditionality is due to the effect of other bodies artificially placed in the flow on the test body in the Ryabushinskii and Zhukov–Roshko models and to the effect of the flow on other sheets of the Riemann surface in the Éfros and Tulin models.

Secondly, the well-known mathematical models ignore the existence of a fluid wake with lost momentum behind the body–cavity system. Thus, the theory loses the feedback which is present in a cavitation flow be-

---

Moscow. Translated from Zhurnal Prikladnoi Mekhaniki i Tekhnicheskoi Fiziki, No. 3, pp. 53–57, May–June, 1987. Original article submitted April 17, 1986.

tween the displacement thickness, momentum thickness, and drag coefficient, preventing an unbounded (in theory) increase in  $c_x$  with an increase in  $Q$ .

The significance of these considerations compels an explanation. This is particularly true in regard to the conditionality of  $c_x$  in the Éfros scheme, where its value can be determined by means of the momentum conservation equation.

1. As is known [5], the use of the momentum conservation equation in the Éfros scheme of cavitation flow about a symmetrical cylindrical body makes it possible to determine the force  $X_J$  acting on the body in a direction coincident with the direction of the velocity of the incoming flow  $v_\infty$ :

$$X_J = \rho q(v_\infty + v_c). \quad (1.1)$$

Here,  $q$  is the rate of flow of the fluid entering the reverse flow per unit of time ( $q = \delta v_c$ ;  $\delta$  is the thickness of the reverse flow);  $v_c$  is the velocity of the fluid at the boundary of the cavity and the reverse flow and is linked with the determining parameter of the problem  $Q$  by a relation which follows from the Bernoulli equation  $v_c/v_\infty = (Q + 1)^{1/2}$ ; the subscript  $J$  indicates that the force  $X$  is determined from the momentum equation.

The quantity  $X$  can be written as the sum of two terms

$$X_J = X_1 + X_2.$$

The first term represents the reaction of a sink of the capacity  $q$  located in an infinite, plane-parallel flow of an incompressible fluid. The second term represents the reactive force of a reverse flow moving counter to the main flow. Thus, Éfros flow about the body is equivalent to a fixed system consisting of a sink receiving fluid from all sides and a reactive nozzle directing fluid into the sink with a constant velocity in one direction — counter to the flow.

Now let us determine the force  $X_E$  acting on this system on the basis of the law of energy conservation: the work of the force  $X_E$  per unit time should be equal to the increment of the kinetic energy of the fluid in the reverse flow corresponding to this time if the system moves with a constant velocity  $v_\infty$  in still fluid away from the system. The increment in the kinetic energy of the reverse flow is equal to  $\rho q(v_\infty + v_c)^2/2$ , so that

$$X_E v_\infty = \rho q(v_\infty + v_c)^2/2,$$

from which

$$X_E = \rho q \frac{(v_\infty + v_c)^2}{2v_\infty}. \quad (1.2)$$

We can obtain the relationship between  $X_E$  and  $X_J$  from (1.1) and (1.2):

$$X_E/X_J = (1 + \bar{v}_c)/2, \quad \bar{v}_c = v_c/v_\infty. \quad (1.3)$$

It can be seen from (1.3) that  $X_E = X_J$  only at  $\bar{v}_c = 1$ , i.e., at  $Q = 0$ . At  $Q \neq 0$ ,  $X_E > X_J$ , and their difference increases with an increase in  $Q$ .

It follows from Galileo's principle that the force  $X_J$  would be invariant in the transition from a coordinate system moving with the system to a coordinate system connected with the quiescent fluid. Thus, it is possible for  $X_J$  and  $X_E$  to be different in the last case only when, along with the work of the force  $X_J$ , there is an additional source of energy  $E_R$  introduced into the system and the energy conservation law must be written as

$$X_J v_\infty + E_R = \rho q(v_\infty + v_c)^2/2.$$

Using (1.1), we determine the additional energy as  $E_R = \rho q(v_c^2 - v_\infty^2)/2$ .

Thus, the work of the force  $X_J$  ensures only the formation of a reverse flow with the velocity  $v_\infty$ , while acceleration of the fluid in this flow from  $v_\infty$  to  $v_c$  occurs as a result of introduction of  $E_R$  from the second sheet of the Riemann surface in the Éfros model. Thus, the force  $X_J$  acting on the body in the Éfros model cannot be regarded as the external drag of the isolated body  $X$ . It is an internal force, as in the Ryabushinskii and Zhukov-Roshko models. In the latter, although flows also occurs on one sheet of the Riemann surface, it forms not an isolated body but a system of bodies which includes additional model bodies.

2. We will examine the need to account for the effect of the displacing action of the wake behind the body-cavity system on the global flow, which determines  $q$  in the reverse flow and, in accordance with (1.1) and (1.2) determines  $X_J$  and  $X_E$  for fixed values of  $v_c$ .

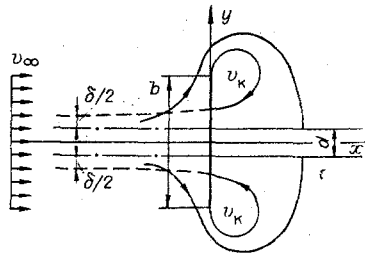


Fig. 1

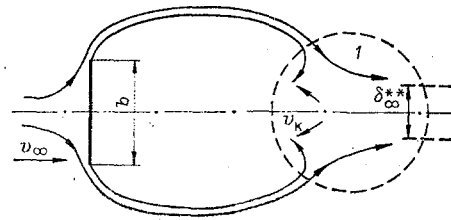


Fig. 2

To account for the effect of the displacing action of the wake on the global flow with a reverse flow, we introduce a new two-parameter flow scheme which differs from the one-parameter Éfros scheme (parameter  $Q$ ) by also including the dependence of the global flow on a second parameter – the displacement thickness of the wake  $d/b$ . The latter is modeled by two plane-parallel plates located symmetrically behind the body (Fig. 1). In this scheme, the reverse flow is split into two individual flows. The total thickness of these two flows away from the body will be designated as  $\delta$ . It is evident that the new two-parameter family of flows is intermediate between the one-parameter family of Éfros flows and the one-parameter (parameter  $\bar{d}$ ) family of Zhukov-Roshko flows. The singularity method of S. A. Chaplygin, used in [5] to find the complex potential for Éfros flow about a flat plate, was also used in [6] to find the complex potential for a new scheme of flow about such a plate, perpendicular to the flow, at an infinitely distant point. The author of [6] also calculated the relation for the thickness of the reverse flow  $\bar{\delta} = f(\bar{d})$  for several values of  $\bar{v}_c = f(Q)$  (Fig. 3 in [6]). At  $\bar{v}_c = 1$  ( $Q = 0$ ), the total thickness of the reverse flow is independent of the displacement thickness of the wake (in this case, an infinitely long cavity minimizes the mutual effect of individual flow regions); however, at  $\bar{v}_c > 1$  ( $Q > 0$ ), the effect of the wake can be evaluated as a first-order effect: with a finite wake displacement thickness  $\bar{d}$ , the thickness of the reverse flow decreases to zero. These values of the parameters  $\bar{v}_c$  and  $\bar{d}$  corresponds to flow by the Zhukovskii-Roshko scheme. Thus, the feedback coupling between the displacement thickness of the wake and the total thickness of the reverse flow, determining the force acting on the plate in accordance with (1.1) and (1.2), actually exists and is strengthened with an increase in  $Q$ .

3. We will theoretically determine the resistance force acting on a flat plate in a cavitation flow as a function of  $Q$ . Above we explained the conditionality of the drag coefficients obtained in well-known steady-state schemes of cavitation flow about bodies and the need to allow for the effect of the displacing action of the wake on the global flow. Figure 2 shows a diagram of actual cavitation flow about a flat plate at  $Q > 0$ . Flow at the end of the cavity (region 1) is nonsteady and of a strongly alternating character: it alternates between flow regimes with a reverse flow and with destruction of the latter (by its mixing with the surrounding liquid). In this region, a large part of the kinetic energy of the fluid of the reverse flow is dissipated and a wake (a region of fluid with lost momentum in the direction of the incoming flow) is formed. The displacing effect of the wake influences the global potential flow.

In the cavitation model of nonsteady flow, we assume that region 1 is characterized in part by dissipation of the entire increment (relative to the still fluid away from the body) of the kinetic energy of the fluid in the reverse flow per unit time  $\rho q (v_\infty + v_c)^2/2$ . Moreover, since (in contrast to the steady flow occurring in the Éfros scheme on two sheets of the Riemann surface) there is no supply of energy  $E_R$ , the only energy source remains the work of the resistance force of the body  $X_E v_\infty$ . Then the law of energy conservation

$$X_E v_\infty = \rho q (v_\infty + v_c)^2/2 \quad (3.1)$$

leads to the expression

$$X_E = \rho q (v_\infty + v_c)^2/2v_\infty, \quad (3.2)$$

which coincides in form with (1.2). However, in (3.2), the thickness of the reverse flow  $\delta = q/v_c$  depends on the displacement thickness of the wake  $\delta_\infty^*$ . Thus, with a fixed value of  $v_c$ ,  $X_E$  is a function only of  $\delta_\infty^*$ . On the other hand, the connection between the resistance force  $X$  acting on the body in an unbounded flow and the momentum thickness of the wake  $\delta_\infty^{**}$  is given by a well-known relation which is also valid for actual cavitation flow:

$$X = \rho v_\infty^2 \delta_\infty^{**} = \rho v_\infty^2 \delta_\infty^* \quad (3.3)$$

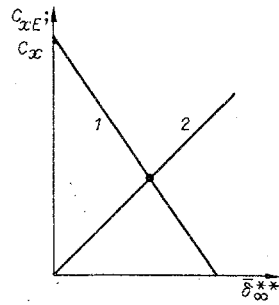


Fig. 3

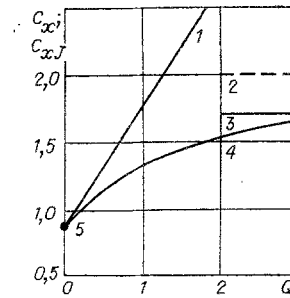


Fig. 4

The closing condition of the model of a second dissipative layer and wake

$$X_E(\delta_{\infty}^*) = X(\delta_{\infty}^*) \quad (3.4)$$

makes it possible to determine  $X$  and  $\delta_{\infty}^*$  with a fixed value of  $v_c$ . Let us reduce (3.2)-(3.4) to dimensionless form

$$c_{xE} = \bar{\delta}(\bar{\delta}_{\infty}^*) \bar{v}_c (1 + \bar{v}_c)^2; \quad (3.5)$$

$$c_x = 2\bar{\delta}_{\infty}^*; \quad (3.6)$$

$$c_{xE}(\bar{\delta}_{\infty}^*) = c_x(\bar{\delta}_{\infty}^*), \quad (3.7)$$

where  $\bar{\delta} = \frac{\delta}{b}$ ;  $\bar{\delta}_{\infty}^* = \frac{\delta_{\infty}^*}{b}$ ;  $\bar{\delta}_{\infty}^{**} = \frac{\delta_{\infty}^{**}}{b}$ ;  $c_x = \frac{2X}{\rho v_{\infty}^2 b}$ ;  $c_{xE} = \frac{2X_E}{\rho v_{\infty}^2 b}$ ;  $b$  is the characteristic dimension of the body.

Figure 3 shows Eq. (3.5) in the plane  $(c_x, c_{xE}; \bar{\delta}_{\infty}^{**})$ . The graph was constructed from the data in Fig. 3 in [6] for flow about a flat plate with the chord  $b$  and a certain prescribed value of  $\bar{v}_c$ . Then the intersection of this relation with the straight line (3.6) satisfies closing condition (3.7) and is the solution of the problem (lines 1 and 2 correspond to  $(c_{xE})_{\bar{v}_c} = \text{const} = f(\bar{\delta}_{\infty}^{**})$ ,  $c_x = 2\bar{\delta}_{\infty}^{**}$ ).

Figure 4 shows the relation for the drag coefficient of a flat plate  $c_x = f(Q)$  obtained by the above method. Also shown for comparison is the familiar relation  $c_{xJ} = f(Q)$  for a flat plate in the case of Éfros flow (lines 4, 1).

It can be seen that at  $Q = 0$  the model of the second dissipative layer and wake and the calculations by the Éfros scheme give identical values of the drag coefficient of a flat plate, coinciding with the classical Kirchhoff result  $c_x = 2\pi/(\pi + 4) \approx 0.88$  (point 5). In the range  $0 < Q \leq 1$  (for which there is experimental data on  $c_x$  for a flat plate), the model function  $c_{xJ} = f(Q)$  deviates and is located below the linear relation  $c_{xJ} = f(Q)$  calculated from the Éfros scheme. The experimental points turn out to be intermediate between these two results. At  $Q > 1$ , the model function  $c_x = f(Q)$  - in contrast to the function  $c_{xJ} = f(Q)$ , which increases without limit with an increase in  $Q$  - asymptotically approaches the finite limit  $c_x = 2.0$  at  $Q \rightarrow \infty$  (line 2).

The existence of a finite limit for the drag coefficient of the plate in the case of cavitation flow [a value which ( $c_x = 2.0$ ) coincides exactly with the empirically well-established drag coefficient for a flat plate in a non-cavitational separated flow in a one-phase fluid] sheds light on the existence of a relationship between cavitation and non-cavitational separated flows. This is shown by the comparison in Fig. 4 of the model function  $c_x = f(Q)$  with the value  $c_x = 1.7 = \text{const}$  (line 3), which was also obtained in [2] with the model of a second dissipative layer and wake for cavitation separated flow of a one-phase incompressible liquid about a plate. The closeness of the model function  $c_x = f(Q)$  at  $Q = 3$  to the model value  $c_x = 1.7$  and the experimental values of  $c_x$  seen for separated flow of a one-phase liquid about a plate, along with the "white spot" observed in experiments with cavitation flow about bodies at  $Q > 1.4$ , makes it possible to conclude that in this range of cavitation numbers, the quasistationary cavity is destroyed and the flow changes to the nonsteady separated flow characteristic of a one-phase liquid.

Thus, the energy approach developed here makes it possible to reliably describe cavitation flow about bodies throughout the range of cavitation numbers from the classical limit ( $Q = 0$ ) to the physical limit at which destruction occurs. Of course, this description cannot be made with the same completeness as is achieved in the mechanical approach (in cases where it can be used). Thus, the energy approach used in the model of a second dissipative layer and wake makes it possible to find the resistance force acting on the body but does not

give information on the distribution of pressure and shear stress on the surface of the body. However, it is better to have a physically reliable value of the drag coefficient of the body and to not know the pressure distribution on it than to have the pressure distribution but to know that it is conditional in character.

#### LITERATURE CITED

1. G. I. Taganov, "Second dissipative layer and wake in viscous flow about a body," Uch. Zap. TsAGI, 1, No. 6 (1970).
2. G. I. Taganov, "Model of circulation near a wing of infinite span with one trailing edge at high Reynolds numbers," Preprint/Division of Mechanics of Inhomogeneous Media, Academy of Sciences of the USSR, No. 5, Moscow (1980).
3. G. I. Taganov, "Substantiation of the relation  $\Pi = \rho v_\infty^2 \delta_{2\infty}^{**}$  used in a model of circulation near a wing of infinite span with a sharp trailing edge," Uch. Zap. TsAGI, 17, No. 5 (1986).
4. C. J. Apelt and C. S. West, "The effects of wake splitter plates on bluff-body flow in the range  $10^4 < R < 5 \cdot 10^4$ . Pt. 2," J. Fluid Mech., 71, Pt. 1 (1975).
5. M. I. Gurevich, Theory of Jets of an Ideal Fluid [in Russian], Nauka, Moscow (1979).
6. V. S. Sadovskii, "Two-parameter family of fluid flows about a plate in the presence of reverse jets," Zh. Prikl. Mekh. Tekh. Fiz., No. 3 (1987).

#### REYNOLDS STRESS DISTRIBUTION DURING LONGITUDINAL FLOW AROUND A DIHEDRAL ANGLE

K. Greichen and V. I. Kornilov

UDC 532.526.4

Study of the structure of so-called complex turbulent flows that cannot be computed sufficiently accurately by methods of the classical theory of a thin shear layer continues to evoke great interest in hydro-aeromechanics. A typical example of shear flows of this kind is the three-dimensional flow along a line of intersection of two surfaces forming a dihedral angle. It is known that similar flows are encountered in different engineering applications, for instance, in the area of wing juncture with the fuselage or other flying vehicle elements, in turbines, and also in prismatic channels.

A whole series of theoretical and experimental researches is devoted to the study of the structure of turbulent flows in angular configurations, in particular, features of the development and interaction of boundary layers [1, 2], the extent of the spatial domain in the transverse direction [2, 3], the secondary flow structure [4], and the influence of different factors on the nature of these complex flows [3, 5]. However, complete information on not only the role of the average velocities but also on the distribution of all the Reynolds stress tensor components is necessary for a correct description of the fundamental physical phenomena in such flows. Similar information is also necessary for further perfection and development of the computation methods, and in particular, for the development of a model of turbulence.

A wide variety of techniques exists for measuring the Reynolds stress component by the hot wire sensor of a thermoanemometer [6]. Analysis of these methods in application to the flow in a dihedral angle shows that the measurement method by a thermoanemometer sensor with a single oblique filament rotating around the housing axis [7] has a number of irrefutable advantages. In particular, it does not require the introduction of any assumptions about the effective velocity in the modified King law, nor also preliminary information about the direction of the stream velocity vector and is released from the necessity to use multichannel apparatus.

Earlier the authors found approval for the mentioned method for the case when the axis of sensor rotation made a right angle with the free stream velocity vector. The maximal error of the Reynolds stress here is on the order of 25-30% of the upper measured value of the appropriate component. It turns out that the fundamental source of errors is due to conditions of aerodynamic sensor interaction with the stream.

---

Berlin. Novosibirsk. Translated from Zhurnal Prikladnoi Mekhaniki i Tekhnicheskoi Fiziki, No. 3, pp. 58-62, May-June, 1987. Original article submitted March 24, 1986.